High ionic conductivity in a $LiFeO_2$-$LiAlO_2$ composite under H_2/air fuel cell condition

Rong Lan and Shanwen Tao*

Department of Chemical & Process Engineering, University of Strathclyde, Glasgow G1 1XJ, UK

Abstract: New ionic conducting materials for electrolytes for electrochemical devices have been attracting the interests of researchers in energy materials. Here, for the first time, we report a conductive composite with high ionic conductivity derived from an electronic conductor α-$LiFeO_2$ and an insulator γ-$LiAlO_2$. High conductivity was observed in α-$LiFeO_2$-γ-$LiAlO_2$ composite when prepared by a solid state reaction method. However, the conductivity enhancement in α-$LiFeO_2$-γ-$LiAlO_2$ composite was not observed when the two oxides were mechanically mixed. The α-$LiFeO_2$-γ-$LiAlO_2$ composite also exhibits O^{2-} or/and H^+ ionic conduction which was confirmed through H_2/air fuel cell measurements. An exceptionally high conductivity of 0.50 S/cm at 650 °C was observed under H_2/air fuel cell condition. This provides a new approach to discover novel ionic conductors from composite materials derived from electronic conductors.

Keywords: Ionic conductor; electronic conductor; composite; conductivity; oxygen ion conductor

---

Introduction

One of the key materials for electrochemical devices is the ionic conducting electrolyte. In search of highly conductive electrolyte materials remains a major task for researchers working on energy materials.[1-4] In this paper, we report the new phenomenon that an

electronic conductor, such as α-$LiFeO_2$ can be converted into an ionic conductor through the formation of a composite with an insulator γ-$LiAlO_2$.

One of the strategies to increase the ionic conductivity of a material is to mix a known ionic conductor with an insulator to form a highly ionic conductive composite. In 1973, Liang reported on enhanced ionic conductivity in AgI-Al_2O_3 composite materials.[5] At 25 °C, the ionic conductivity of the composite with 35-45mol% Al_2O_3 (10^{-5} S/cm) is two orders of magnitude higher than that of pure AgI (10^{-7} S/cm).[5] Following this pioneer work, many papers have been published on ionic conducting materials based on salt-oxide composites, such as CuCl-Al_2O_3[6, 7], CaF_2-Al_2O_3[8], AgBr-Al_2O_3,[9, 10] LiBr-Al_2O_3,[11] lithium halide-based quaternary compounds,[12] Li_2SO_4-Al_2O_3[13] and other systems.[14] J. Maier made a comprehensive research on the conduction mechanism of the salt-oxide composite materials and the enhanced ionic conductivity is attributed to the defects in the space charge layer at the salt-oxide interfaces.[15-17] He also emphasised that the implementation of a high density of interfaces can lead to a substantial impact on the overall or even local ionic transport properties of solids.[18] The development of ionic-conducting composite materials has been reviewed in several papers.[18-24]

As for electrolyte materials for solid oxide fuel cells (SOFCs), the existing typical electrolytes such as yttrium stabilised zirconia (YSZ), gadonilium doped ceria (GDC), Sr- and Mg-doped $LaGaO_3$ (LSGM) and Y-doped $BaCeO_3$/$BaZrO_3$ are good but also have drawbacks, such as poor mechanical strength, too expensive or with insufficient conductivity at intermediate temperature (500 -700 °C).[1, 25] Low cost conductive electrolyte materials for intermediate temperature solid oxide fuel cells (IT-SOFCs) are still in high demand. Therefore to developed ionic conducting electrolytes based on composite materials taking advantage of the interface effects is a good strategy.[18]

There are some reports on ionic conductivity of oxide-oxide composite materials. Researchers tried to discover a good electrolyte in composite materials for high temperature electrochemical devices. It has been reported the 3mol% yttria stabilised zirconia (3YSZ) – MgO composite exhibits a lower conductivity at a temperature below 700 °C,[26] the conductivity of 8YSZ-Al_2O_3 composite is lower than pure 8YSZ.[27] Addition of Al_2O_3 in doped CeO_2 causes increased grain boundary resistance thus reduced total

conductivity.[28] The conductivity of $La_{0.9}Sr_{0.1}Ga_{0.8}Mg_{0.2}O_{2.85}$ (LSGM) and $Ce_{0.8}Sm_{0.2}O_{1.9}$ (SDC) composite with a LSGM to SDC weight ratio of 1:9 exhibits slightly higher conductivity than both LSGM and SDC at a temperature below 650 °C.[29] Zhu et al. reported that high ionic conductors can be obtained in the samarium doped ceria (SDC) and lithium doped ZnO (Li_xZnO) composite with a core-shell microstructure with ionic conductor SDC as the core, electronic conductor Li_xZnO as the shell. This electrolyte exhibits super-ionic conductivity (> 0.1 S cm^{-1} over 300 °C).[30, 31] The same author also reported that maximum conductivity (about 1.0 S cm^{-1}) was obtained for the optimized Y_2O_3-SDC composite electrolyte at 600 °C.[32] The effects on conductivity enhancement in composite oxides is mixed. In most cases, the conductivities of composites are lower than that of the starting components. Conductivity enhancement was also observed in some systems.

Recently we reported the high protonic conductivity in layered oxide $Li_xAl_{0.5}Co_{0.5}O_2$ with a proton conductivity of 0.10 S/cm at 500 °C.[33, 34] This inspired us to developed proton-conducting electrolyte in other layered oxide such as γ-$LiFeO_2$.[35] In our experiment, it was found that new oxide with nominal composition '$LiFe_{0.7}Al_{0.3}O_2$' was actually a mixture of α-$LiFeO_2$ and γ-$LiAlO_2$ when prepared by a solid state reaction method (Figure 1A). Further experiments indicated that the as-prepared $LiFeO_2$-$LiAlO_2$ composite not only exhibits high conductivity, but exhibits O^{2-}/H^+ ionic conduction under a H_2/air fuel cell condition. $LiFeO_2$ has been investigated to be used as potential cathode for molten carbonate fuel cells (MCFCs) due to its electronic conduction but its application is limited to the low conductivity.[36] $LiAlO_2$ is an insulator widely used as the electrolyte matrix for MCFCs.[28] Our experiments indicate that a good ionic conductor can be derived from an electronic conductor such as α-$LiFeO_2$ through the formation of a composite with an insulator such as γ-$LiAlO_2$. In this paper, for the first time, a highly conductive composite $LiFeO_2$-$LiAlO_2$ and its conduction behaviour have been investigated. It should be noted that, due to the sublimation of lithium during the preparation process, all the oxide materials presented in this work are likely to be lithium deficient.

Results and discussion

Phase composition and conductivity of $LiFeO_2$-$LiAlO_2$ composite

Figure 1A shows the XRD pattern of the sample after firing at 900 °C for 1 hour. Instead of forming a single phase layered oxide, the as-prepared material contains cubic α-$LiFeO_2$ and tetragonal γ-$LiAlO_2$ with a trace amount of unreacted Li_2CO_3 (PDF No. 80-1307). The lattice parameters of the two phases are listed in Table 1. Reports on new phases between the $LiFeO_2$ and $LiAlO_2$ system are scarce. One of the possible reasons is that $LiFeO_2$ and $LiAlO_2$ do not form solid solution phases or the solubility limits are very low in either phase. In our experiments, it has been demonstrated that the as-prepared sample is mainly a mixture of two oxides. The cross-section of the $LiFeO_2$-$LiAlO_2$ composite pellet indicated that it is composed of particles with particle size ranged between 5 - 20 μm (Figure 2A). Energy dispersive spectroscopy (EDS) analysis further confirms that it is a composite of two oxides. It has been reported that γ-$LiAlO_2$ can be doped by 2mol% Fe at the Al-site.[37] Therefore the γ-$LiAlO_2$ phase will be doped with a small amount of Fe and vice versa. The doping level of Fe in $LiAlO_2$ and Al in $LiFeO_2$ seems quite low (Figure S1). Lithium was not observed in the EDS spectrum because its atomic number is too low to be detected by EDS.

γ-$LiAlO_2$ has been reported as a good promoter for ionic conductor in the salt-oxide composite materials. It has been reported that addition of γ-$LiAlO_2$ in the $LiClO_4$-$LiAlO_2$ composites can significantly increase the Li^+ ion conductivity.[38] It would be interesting to investigate the conductivity of $LiFeO_2$-$LiAlO_2$ composite to see if the conductivity of $LiFeO_2$ can be enhanced too. At 700 °C in air, it was found that the total conductivity was 0.48 S/cm but slightly decreased to 0.47 S/cm after 135 minutes (Figure 3A). The possible reason for the slight decrease of conductivity is due to the change of local defects and defect concentration at the $LiFeO_2$-$LiAlO_2$ interface when ageing at 700 °C if the total conductivity is closely related to the defects at this interface.[15] The conductivity was quite stable at 700 °C. The total conductivity was over 0.10 S/cm at a temperature above 600 °C.

Some of the typical a.c. impedance spectra of the $LiFeO_2$-$LiAlO_2$ composite in air are shown in Figure 4. The obvious depressed semi-circles for electrode responses at lower frequencies indicates it could be an ionic conductor or a semi-conductor. For impedance patterns recorded at 700 °C, the normalized capacitor of the semi-circle was ~ 10^{-2} F/cm indicating

that the semi-circle was the response of electrode thus only the total resistance was measured.[39] However, at reduced temperature, for the impedance response at middle frequency at 610 °C and high frequency at 512 °C (Figures 4C&D, the corresponding capacitor was in the range of ~ 10^{-8} F/cm indicating it was the response of grain boundary.[39] The conductivity displayed in Figure 3 for $LiFeO_2$-$LiAlO_2$ composite was the total conductivity. Thermogravimetric (TG) analysis of the $LiFeO_2$-$LiAlO_2$ composite in air indicated slow weight loss starting from 600 °C (Figure 5). This is more likely due to the loss of oxygen from the two oxides, particularly $LiFeO_2$. The melting point of Li_2CO_3 is 723 °C. Evaporation of the trace amount of Li_2CO_3 cannot be ruled out. TG analysis of the composite sample in 5%H_2/Ar indicated slight weight loss starting from 50 °C and this became more significant at a temperature above 500 °C (Figure 5). Besides the possible desorption of water and gases, it is more likely that H_2 interacted with the material therefore caused the loss of oxygen from either $LiFeO_2$ particles or the grain boundary, forming either reduced $LiFeO_{2-\delta}$ or oxygen vacancies at the grain boundary. This is also reflected on the conductivity change of $LiFeO_2$-$LiAlO_2$ composite in 5%H_2/Ar (Figure 3A). At 700 °C, the initial conductivity of the $LiFeO_2$-$LiAlO_2$ composite in 5%H_2/Ar almost equals to that in air. It gradually increased to 0.51 S/cm after 1 hour then gradually decreased then tended to be stable at 0.34 S/cm after 8 hours. The further reduction of the composite may lead to increased concentration in oxygen vacancies. It has been reported that, for YSZ, the oxygen ionic conductivity decreases at high doping level because oxygen vacancy clusters may be formed at high concentration of oxygen vacancy leading to reduced oxygen ionic conductivity.[40] Similar situation may happen in the $LiFeO_2$-$LiAlO_2$ composite in this study. The possible reduction of $LiFeO_2$-$LiAlO_2$ composite reached an equilibrium after held at 700 °C for a period of time thus the conductivity tended to be stable. Conductivity measurements on cooling of the composite indicated the conductivity in 5%H_2/Ar is lower than that in air (Figure 3B) in the measured temperature range. The typical a.c. impedance spectra of the sample in 5%H_2/Ar are shown in Figure 6. It was found that the response at middle frequency (~ 10 kHz) became larger against time. The corresponding capacitor decreased from 10^{-2} to 10^{-5} F/cm during the measured 8 hours. The small depressed semi-circle at middle frequency is likely due to the responses of electrolyte/electrode interfaces. The increased resistance in electrolyte/electrode interfaces also led to increased total resistance, thus decreased total conductivity against time in 5%H_2/Ar (Figure 3A). The increased electrolyte/electrode

interface resistance was not observed during the conductivity measurement in air (Figures 4A&B) indicating there are interactions between $LiFeO_2$-$LiAlO_2$ composite or silver electrode and H_2 and further investigation is required. Another possible reason is due to the exsolution of Li_2CO_3 during the conductivity measurements (Figure 1B). The exsolved Li_2CO_3 may diffuse to the surface of the electrolyte which caused the change of electrolyte/electrode interface. It should be noted that the change of electrolyte/electrode interface is significant in 5%H_2/Ar while it is insignificant in air (Figures 4A and 6A). Thus this change is related to the presence of H_2, most likely related to the loss of oxygen in $LiFeO_2$ which is discussed in details below.

It has been observed that the conductivities of $LiFeO_2$-$LiAlO_2$ composite in both air and 5%H_2/Ar are roughly two and four orders of magnitude greater than the reported values of pure $LiFeO_2$ [36]and γ-$LiAlO_2$[41] respectively (Figure 3B). The conductivity of $LiFeO_2$-$LiAlO_2$ composite is also roughly 1-2 orders of magnitude higher than that for pure Li_2CO_3.[42] It has been reported that the conductivity of Li_2CO_3-γ-$LiAlO_2$ composite with 40 vol% Li_2CO_3 is lower than 0.1 S/cm below the melting point of Li_2CO_3, 723 °C.[43] Therefore the observed conductivity enhancement in the $LiFeO_2$-$LiAlO_2$ composite is unlikely related to the presence of Li_2CO_3 itself. The possible reason is the enhancement effects in composite materials as the case for $LiClO_4$/γ-$LiAlO_2$ composites.[38] Another possibility is the formation of lithium rich oxides. Although it was found that Li-rich γ-$LiAlO_2$ is more conductive[41] but it is unlikely in our study as no access Li_2CO_3 was added in the precursors while there are a tiny amount of Li_2CO_3 left in the produced composite (Figure 1A). After the conductivity measurements, the $LiFeO_2$-$LiAlO_2$ composite was cooled down in 5%H_2/Ar. XRD pattern indicated that the composite still remained the same phase but more Li_2CO_3 peaks appear, possibly due to crystallisation of amorphous Li_2CO_3 or exsolution of Li2CO3 from the $LiFeO_2$-$LiAlO_2$ composite after experiencing high temperature measurements (Figure 1B).

In order to further confirm this observed conductivity enhancement in $LiFeO_2$-$LiAlO_2$ composite, pure α-$LiFeO_2$ were prepared by a similar solid state reaction method using the same precursor. A commercial γ-$LiAlO_2$ (Alderich) was directly used for preparation of pellet for conductivity and other measurements. It was found that the conductivity of γ-$LiAlO_2$ in our experiment is very close to the reported value (Figure 3B). The conductivity of α-$LiFeO_2$

is in the same range with the reported value for $LiFeO_2$ although it was unclear which phase it was.[36] The conductivity of the mechanically mixed $LiFeO_2$-$LiAlO_2$ lies between pure $LiFeO_2$ and $LiAlO_2$ (Figure 3B). This experiment indicates that the conductivity enhancement in the $LiFeO_2$-$LiAlO_2$ composite only happens when the composite was prepared simultaneously in the same batch. This makes the composite have the best homogeneity and fine grain boundaries are formed between $LiFeO_2$ and $LiAlO_2$ particles. Conductivity enhancement was not observed in mechanically mixed $LiFeO_2$-$LiAlO_2$ (Figure 3B).

O^{2-} and H^+ ion conduction in the $LiFeO_2$-$LiAlO_2$ composite

O_2 and H_2 concentration cells were used to figure out the possible O^{2-} or H^+ conduction of the $LiFeO_2$-$LiAlO_2$ composite.[33] Oxygen concentration cell measurement indicated the material may exhibit some kind of O^{2-} conduction (Figure 7A). It is hard to explain that, on cooling, the observed OCV between 575 and 475 °C is slightly higher than the theoretical values. One possible reason is the local chemical composition difference of the composite exposing in O_2 and air sides. In general, the transfer number for O^{2-} ion conduction is not high under the O_2/air concentration cell condition indicating that it is not a pure O^{2-} ionic conductor. The decreased OCVs on both heating and cooling at higher temperature in the oxygen concentration cell (Figure 7A) is opposite to those calculated from Nernst equation. This is very complicated, besides the difference in local chemical composition, in the presence of Li^+ and other ions, the gathering of certain cations, say Li^+ ions, and anions other than O^{2-} ions, say, CO_3^{2-} ions from exsolved Li_2CO_3, at the electrolyte/electrode interfaces may also cause potential difference. It cannot be unambiguously concluded that the $LiFeO_2$-$LiAlO_2$ composite exhibits O^{2-} conduction under the oxygen concentration cell measuring conditions. The observed OCV was close to zero in hydrogen concentration cell measurement indicated that the composite exhibits negligible proton conduction (Figure 7B) under the hydrogen concentration cell measuring conditions. This phenomenon is very different from the proton conduction in layered oxide $Li_xAl_{0.5}Co_{0.5}O_2$ [33] because the α-$LiFeO_2$ phase in the composite exhibits cubic disordered rock salt structure which is not a layered oxide.[35] The potential mobile channels for protons in layered oxides do not exist in the cubic α-$LiFeO_2$. It should be noted that proton conduction has been widely reported in

materials which are not with layered structure. The layered structure may facilitate the mobility of protons but this is not essential in proton-conducting materials such as those with perovskite or scheelite structures.[44, 45] Besides the possible O^{2-} ion conduction, the measured total conductivity of $LiFeO_2$-$LiAlO_2$ composite in both air and 5%H_2/Ar may contain Li^+ ions and electronic conduction.

The open circuit voltage (OCV) of a H_2/O_2 cell of the cell is shown in Figure 7C. An OCV of 0.3 V was observed at 300 °C and gradually increased to 0.85 V at 600 °C which is comparable to the OCV for hydrogen fuel cells based on doped CeO_2 electrolyte.[46] The observed OCV is lower than theoretical OCV for a H_2/air fuel cell (~ 1.0V) indicating that the $LiFeO_2$-$LiAlO_2$ composite is not a pure O^{2-}/H^+ conductor and it also exhibits Li^+ or/and electronic conduction under the H_2/air fuel cell conditions. At a temperature around 600 °C, the O^{2-}/H^+ conduction became significant.

The high observed OCV under H_2/O_2 fuel cell conditions might be related to the reduction of $LiFeO_2$ phase. $LiAlO_2$ has been used as matrix in MCFC and demonstrated stable in the presenc of H_2 at high temperature. Under the H_2/O_2 fuel cell conditions, $LiFeO_2$ was reduced to oxygen deficient $LiFeO_{2-\delta}$ also forming oxygen vacancies.

$$LiFeO_2 \rightarrow LiFeO_{2-\delta} + \delta/2\, O_2 \qquad (1)$$

For charge balance, the charge for iron ions will change from 3+ to 2+. If the iron is at low spin, then the energy level configurations for iron ions are as follows: Fe^{2+}, $t_{t_g}^6 e_g^0$; Fe^{3+}, $t_{t_g}^5 e_g^0$.[47] The Fe^{2+} ions will be an insulator at low spin because there are no unpaired electrons. Under the circumstance, electronic conductor $LiFeO_2$ will be converted into an ionic conductor $LiFeO_{2-\delta}$. In the case of pure $LiFeO_2$, only part of Fe^{3+} ions in $LiFeO_2$ are reduced to Fe^{2+} ions, thus it is still dominated by electronic conduction therefore no OCV was observed on the H_2/air fuel cell using pure $LiFeO_2$ as the electrolyte. In the $LiFeO_2$-$LiAlO_2$ composite, the existence of the unique interface may partially block the pathway for electrons thus high OCV was observed. The simultaneously formed oxygen vacancies may lead to oxygen ion conduction in the $LiFeO_2$-$LiAlO_2$ composite, as the case for typical oxygen

ion conductors such as YSZ, SDC.[48] From this point of view, $LiFeO_2$-$LiAlO_2$ composite is likely an O^{2-} ionic conductor under the H_2/O_2 fuel cell conditions. On the other hand, protons may also transfer through the oxygen vacancies as the case in doped perovskite oxides such as doped $BaCeO_3$, $BaZrO_3$ and $LaGaO_3$.[1, 44, 49, 50] Then $LiFeO_2$ is a potential proton conductor as well. In both case, the reduction of $LiFeO_2$ in the presence of H_2 is the key to trigger the ionic conduction. Although the cell voltage in the hydrogen concentration cell is quite low (Figure 7B), the $LiFeO_2$-$LiAlO_2$ composite may still exhibit proton conduction because the driving force (potential difference) in a H_2/O_2 fuel cell is nearly 10 times of that for a hydrogen concentration cell. In a previous study on $Li_xAl_{0.5}Co_{0.5}O_2$, the measured transfer number for protons through hydrogen concentration cell was also lower than that from a H_2/air fuel cell.[33]

Under the H_2/O_2 fuel cell conditions, it is likely that $LiFeO_2$-$LiAlO_2$ composite is a mixed O^{2-}/H^+ conductor, together with some level of electronic conduction because the observed OCV was still lower than theoretical values. γ-$LiAlO_2$ has been used as electrolyte matrix in molten carbonate fuel cells indicating it is stable in hydrogen at high temperature. The conductivity of $LiAlO_2$ is very low and is expected not to change in the presence of hydrogen. The conductivity enhancement from the co-existed γ-$LiALO_2$ phase in the $LiFeO_2$-$LiAlO_2$ composite is expected negligible. Therefore the conductivity enhancement is likely due to both the unique $LiFeO_2$-$LiAlO_2$ interface and the reduction of $LiFeO_2$ phase. Simple reduction of $LiFeO_2$ cannot block the pathways for electrons to create ionic conductor as no OCV was observed in a H_2/air fuel cell using pure $LiFeO_2$ as the electrolyte.

These experiments demonstrated that, in the presence of hydrogen, the $LiFeO_2$-$LiAlO_2$ composite can potentially exhibit both O^{2-} and H^+ ionic conduction at evaluated temperatures. The possible pathway is through the oxygen vacancies in reduced α-$LiFeO_2$ and the defects in the α-$LiFeO_2$/γ-$LiAlO_2$ interface.

To further confirm the possible O^{2-}/H^+ conduction of the α-$LiFeO_2$-γ-$LiAlO_2$ composite, a cell with thickness of 0.8 mm was used for H_2/air fuel cell measurements. The OCV of the cell at different temperatures is shown in Figure 8. High OCV around 0.95 V was observed at a temperature above 600 °C. The OCV was unstable because the O^{2-}/H^+ ionic conduction is

closely related to the reduction of Fe^{3+} ions. The more Fe^{2+} ions in the $LiFeO_{2-\delta}$, the higher the OCV. Figure 9A shows the fuel cell performance at 650 °C for four runs. The power densities increased at the first three runs which is related to the activation effects for SOFCs. An OCV above 0.9 V with maximum power density of 45 mW/cm^2 was achieved. As shown in Figure 9A, The I-V and I-P curves are not smooth as normally observed in other studies. As the ionic conduction is dominated by the Fe^{3+}/Fe^{2+} redox cycling, at different cell voltages, the driving force for O^{2-} and H^+ ions is different. For example, at low cell voltage or low driving force, the proton conduction would be quite small as has been confirmed through hydrogen concentration cell measurement (Figure 7B). The two peaks on the I-P curves at the 3rd and 4th run in Figure 9A may reflect the types of dominated charge carriers, say, O^{2-} and H^+ ions. It is speculated that the $LiFeO_2$-$LiAlO_2$ composite is dominated by proton conduction at high cell voltage and O^{2-} ions at intermediate voltage. The fuel cell performance was also measured on cooling between 650 and 600 °C. The OCV was ~ 0.9 V at 625 °C but dropped to 0.75 V at 600 °C. The a.c. impedance spectra of the cell measured at OCV are shown in Figure 10. It can be seen that the polarisation resistance of the electrode is quite high due to the use of un-optimised Ag electrode. However, the normalised series resistance was 0.33, 0.29 and 0.16 Ωcm^2, corresponding to a conductivity of 0.24, 0.28 and 0.50 S/cm at 600, 625 and 650 °C respectively. This is comparable to the conductivity than the α-$LiFeO_2$/γ-$LiAlO_2$ composite measured in air (Figure 3B). Under the H_2/air fuel cell condition, the driving force between anode and cathode may make the O^{2-}/H^+ ions moving faster in $LiFeO_2$ or at the interface of the composite, leading to higher conductivity. The high OCV of the H_2/air fuel cell indicates the conductivity is dominated by O^{2-}/H^+ conduction. The observed conductivity in the H_2/air fuel cell is comparable to the measured conductivity of the composite in air or 5%H_2/Ar (Figure 3B). The high potential difference or driving force in H_2/air fuel cell compared to those in the H_2 or O_2 concentration cells may increase the mobility of O^{2-} (or H^+) ions in $LiFeO_2$ or along the grain boundary, i.e., the interface, resulting in an exceptionally high ionic conductivity.

This experiment indicates that, at a temperature above 600 °C, under the H_2/air fuel cell condition, the α-$LiFeO_2$-γ-$LiAlO_2$ composite is dominantly an O^{2-}/H^+, probably an O^{2-} ion conductor. After the fuel cell measurements, the cross-section of the pellet was still dense

(Figure 2B). The composition kept unchanged but the Li_2CO_3 peak becomes stronger, possibly due to crystallisation of the amorphous Li_2CO_3 or exsolution of Li_2CO_3 from the composite (Figure 1C). The lattice volumes of both α-$LiFeO_2$ and γ-$LiAlO_2$ lies between the original and those after the conductivity measurement (Table 1). This is understandable as the whole composite was exposed in 5%H_2/Ar at high temperature for a long time during the conductivity measurement while only the anode was exposed in H_2 during the fuel cell measurements.

Conclusions

In conclusion, exceptionally high conductivity was observed in the α-$LiFeO_2$/γ-$LiAlO_2$ composite. The conductivity of composite is orders of magnitude higher than that for pure $LiFeO_2$ or $LiAlO_2$. However, the conductivity enhancement in α-$LiFeO_2$/γ-$LiAlO_2$ composite was not observed when the two oxides were mechanically mixed. The exceptional high conductivity is likely related to the reduction of $LiFeO_2$ and the fine grain boundary when prepared by a direct synthesis process. It should be noted that the measured high total conductivity for α-$LiFeO_2$-γ-$LiAlO_2$ composite in air and 5%H_2/Ar may contain Li^+ ions, O^{2-}/H^+ ions even electronic conduction. Under a H_2/air fuel cell condition, ionic conductivity of 0.24 ~ 0.50 S/cm was observed between 600 and 650 °C. The high OCV together with obvious current observed at a temperature ~ 600 °C indicated that the α-$LiFeO_2$-γ-$LiAlO_2$ composite is a dominant O^{2-}/H^+ conductor under H_2/air fuel cell conditions. This study indicates that super-ionic conductors can be obtained in a composite materials derived from an electronic conductor such as $LiFeO_2$ and an insulator $LiAlO_2$. This will provide a new approach to discover novel ionic conducting materials to be used as electrolyte for electrochemical devices, such as fuel cells, hydrogen separation cells if the proton conductivity is high enough. However, the high O^{2-}/H^+ ionic conductivity only happens at a narrow temperature range with high OCV in a H_2/air fuel cell which may limit its application therefore better composite ionic conductors are to be discovered for real applications.

Experimental Section

Preparation of $LiFeO_2$-$LiAlO_2$ composite

The $LiFeO_2$-$LiAlO_2$ composite material was prepared by a solid state reaction method. Li_2CO_3, Fe_2O_3 and Al_2O_3 (all from Alfa Aesar) were dried at 500 °C for a couple of hours to remove the adsorbed water. Calculated amounts of Li_2CO_3, Fe_2O_3 and Al_2O_3 with Li:Fe:Al molar ratio of 1:0.7:0.3 was weighed and ball-milled for 60 minutes at 400 rpm in a FRITSCH P6 miller using a zirconia container with zirconia balls. After firing at 800 °C for 24 hours, the mixture was pressed into pellets with diameter of 13mm and 20 mm, then fired at 900 °C for 1 hour. The as-prepared pellets were used for conductivity and electrochemical measurements.

For synthesis of α-$LiFeO_2$, Li_2CO_3 and Fe_2O_3 were dried at 500 °C for a couple of hours to remove the adsorbed water. Stoichiometric amounts of Li_2CO_3 and Fe_2O_3 with Li:Fe molar ratio of 1:1 was weighed and ball-milled for 60 minutes at 400 rpm in a FRITSCH P6 miller using a zirconia container with zirconia balls. After firing at 800 °C for 24 hours, the mixture was pressed into pellets with diameter of 13mm and 20 mm, then fired at 900 °C for 1 hour. The as-prepared pellets were used for conductivity and electrochemical measurements.

A commercial γ-$LiAlO_2$ (Alderich) was directly used to press into pellets with diameter of 13mm and 20 mm, then fired at 1100 °C for 4 hour. The as-prepared pellets were used for conductivity and electrochemical measurements.

The mechanically mixed α-$LiFeO_2$-γ-$LiAlO_2$ pellets was prepared by mixing the as-prepared pure α-$LiFeO_2$ and commercial γ-$LiAlO_2$ at a molar ratio of α-$LiFeO_2$ to γ-$LiAlO_2$ at 7:3. The mixture was ball-milled for 60 minutes at 400 rpm in a FRITSCH P6 miller using a zirconia container with zirconia balls. It was then pressed into pellets with diameter of 13mm, then fired at 900 °C for 1 hour. The as-prepared pellets were used for conductivity measurements.

The relative density of both α-$LiFeO_2$-γ-$LiAlO_2$ composite and mechanically mixed pellets was estimated around 90%.

Materials characterisation

X-ray data were collected on a PANanalyticalX'Pert Pro in the Bragg-Brentano reflection geometry with a Ni-filtered Cu Kα source (1.5405 Å), fitted with an X'Celerator detector and an Empyrean CuLFF xrd tube. Absolute scans in the 2θ range of 5-100° with step sizes of 0.0167º were used during data collection.

Thermal analyses of sample nominal composition '$LiFe_{0.7}Al_{0.3}O_2$' were carried out in air and 5%H_2/Ar using a Stanton Redcroft STA/TGH series STA 1500 operating through a Rheometric Scientific system interface controlled by the software RSI Orchestrator in flowing compressed air and 5% H_2/Ar at a flow rate of 50 ml/min.

SEM observation was carried out on a HITACHI SU-6600 Field Emission Scanning Electron Microscope (FE-SEM). The FE-SEM is equipped with Energy Dispersive Spectroscopy (EDS), Oxford Inca 350 with 20mm X-Max detector plus software to allow elemental analyses of metals and ceramic materials.

Conductivity measurements

The pellets with diameter of ~ 13mm and thickness of 2-3mm were used for conductivity measurements. It was found that platinum may react with the Li-containing materials.[33] Therefore silver paste was coated on both sides of the pellets and dried under UV lamp, fired at 700 °C for 1 hour before conductivity and electrochemical testing. The a.c. conductivity of pure $LiFeO_2$, $LiALO_2$, $LiFeO_2$-$LiAlO_2$ composite with nominal composition '$LiFe_{0.7}Al_{0.3}O_2$' and the $LiFeO_2$-$LiAlO_2$ mixture in air was measured on cooling measured by a Solartron 1470E/1455 with applied frequency from 1MHz to 0.01Hz. The sample pellets were coated with silver paste and fired at 700 °C for 30 minute the measurements were

carried out in static air. For the $LiFeO_2$-$LiAlO_2$ composite, conductivity in dry 5%H_2/Ar (passing through room temperature 95% H_2SO_4) was also measured following the conductivity measurements in air.

O_2 and H_2 concentration cell measurements

For concentration cell measurement, the pellets of pure $LiFeO_2$, $LiAlO_2$ and $LiFeO_2$-$LiAlO_2$ composite with composition '$LiFe_{0.7}Al_{0.3}O_2$' was coated with diluted silver paste on both sides and fired at 700 °C for 1 hour. The diameter of pellets for concentration and fuel cell measurements was around 20mm. The thickness was 0.8 mm with active area for the cell was ~ 0.6 cm^2.

For oxygen concentration cell, air and pure oxygen were passing through 95% H_2SO_4 respectively before feeding into the two chambers of the cell. For hydrogen concentration cell, 5%H_2/Ar and pure hydrogen were passing through 95% H_2SO_4 respectively before feeding into the two chambers of the cell. The voltage of the cell was recorded on a Solartron 1470E electrochemical interface.

H_2/air fuel cell measurements

Pellets of $LiFeO_2$-$LiAlO_2$ composite with thickness of 0.8mm with active area of 0.6 cm^2 was used for H_2/air fuel cell measurements. Pure silver paste was used as both anode and cathode. The cells were mounted on an alumina tube using a ceramic sealant for sealing.[51] Hydrogen passing room temperature water was fed inside the tube and the cathode was exposed to open air. The flow rate of hydrogen was 50 ml/min. The a.c. impedance at OCV and I-V curve of the cell were recorded by a Solartron 1470E/1455 electrochemical interface.

Acknowledgements

The authors thank EPSRC Flame SOFCs (EP/K021036/1), UK-India Biogas SOFCs (EP/I037016/1) and SuperGen Fuel Cells (EP/G030995/1) projects for funding.

References

[1] B. C. H. Steele, A. Heinzel, *Nature* **2001**, *414*, 345-352.
[2] J. M. Tarascon, M. Armand, *Nature* **2001**, *414*, 359-367.
[3] S. Wang, Y. Chen, S. Fang, L. Zhang, M. Tang, K. An, K. S. Brinkman, F. L. Chen, *Chem. Mater.* **2014**, *26*, 2021–2029.
[4] K. Fujii, Y. Esaki, K. Omoto, M. Yashima, A. Hoshikawa, T. Ishigaki, J. R. Hester, *Chem. Mater.* **2014**, *26*, 2488–2491.
[5] C. C. Liang, *J. Electrochem. Soc.* **1973**, *120*, 1289-1292.
[6] M. R. W. Chang, K. Shahi, J. B. Wagner, *J. Electrochem. Soc.* **1984**, *131*, 1213-1214.
[7] T. Jow, J. B. Wagner, *J. Electrochem. Soc.* **1979**, *126*, 1963-1972.
[8] S. Fujitsu, M. Miyayama, K. Koumoto, H. Yanagida, T. Kanazawa, *J. Mater. Sci.* **1985**, *20*, 2103-2109.
[9] J. Maier, *Phys. Status Solidi B-Basic Res.* **1984**, *123*, K89-K91.
[10] J. Maier, *Mater. Res. Bull.* **1985**, *20*, 383-392.
[11] O. Nakamura, J. B. Goodenough, *Solid State Ionics* **1982**, *7*, 119-123.
[12] P. Hartwig, W. Weppner, *Solid State Ionics* **1981**, *3-4*, 249-254.
[13] B. Zhu, Z. H. Lai, B. E. Mellander, *Solid State Ionics* **1994**, *70*, 125-129.
[14] F. W. Poulsen, N. H. Andersen, B. Kindl, J. Schoonman, *Solid State Ionics* **1983**, *9-10*, 119-122.
[15] J. Maier, *J. Electrochem. Soc.* **1987**, *134*, 1524-1535.
[16] J. Maier, *J. Phys. & Chem. Solids* **1985**, *46*, 309-320.
[17] J. Maier, *Phys. Status Solidi B-Basic Res.* **1984**, *123*, K89-K91.
[18] J. Maier, *Nat. Mater.* **2005**, *4*, 805-815.
[19] R. C. Agrawal, R. K. Gupta, *J. Mater. Sci.* **1999**, *34*, 1131-1162.
[20] S. W. Tao, D. K. Peng, G. Y. Meng, *J. Inorg. Mater.* **1999**, *14*, 203-210.
[21] P. Knauth, *J. Electroceramics* **2000**, *5*, 111-125.
[22] N. F. Uvarov, *J. Solid State Electrochem.* **2011**, *15*, 367-389.
[23] A. B. Yaroslavtsev, *Inorg. Mater.* **2012**, *48*, 1193-1209.
[24] L. Fan, C. Wang, M. Chen, B. Zhu, *J. Power Sources* **2013**, *234*, 154-174.
[25] M. Li, M. J. Pietrowski, R. A. De Souza, H. Zhang, I. M. Reaney, S. N. Cook, J. A. Kilner, D. C. Sinclair, *Nat. Mater.* **2014**, *13*, 31-35.
[26] Y. Shiratori, F. Tietz, H. P. Buchkremer, D. Stover, *Solid State Ionics* **2003**, *164*, 27-33.
[27] F. Yang, X. Zhao, P. Xiao, *Solid State Ionics* **2010**, *181*, 783-789.
[28] Y. J. Kang, H. J. Park, G. M. Choi, *Solid State Ionics* **2008**, *179*, 1602-1605.
[29] S. Li, Z. Li, B. Bergman, *J. Alloys & Compds* **2010**, *492*, 392-395.
[30] L. Fan, Y. Ma, X. Wang, M. Singh, B. Zhu, *J. Mater. Chem. A* **2014**, *2*, 5399-5407.
[31] J. S. Wu, B. Zhu, Y. Q. Mi, S. J. Shih, J. Wei, Y. Z. Huang, *J. Power Sources* **2012**, *201*, 164-168.
[32] R. Raza, G. Abbas, X. Wang, Y. Ma, B. Zhu, *Solid State Ionics* **2011**, *188*, 58-63.
[33] R. Lan, S. W. Tao, *Adv. Energy Mater.* **2014**, *4*, 1301683.
[34] R. Lan, S. W. Tao, *ChemElectroChem* **2014**, *in press*, DOI: 10.1002/celc.201402102.
[35] M. Holzapfel, C. Haak, A. Ott, *J. Solid State Chem.* **2001**, *156*, 470-479.
[36] C. E. Baumgartner, R. H. Arendt, C. D. Iacovangelo, B. R. Karas, *J. Electrochem. Soc.* **1984**, *131*, 2217-2221.
[37] N. Suriyamurthy, B. S. Panigrahi, A. Natarajan, *Mater. Sci. & Eng. A-Structural Mater. Properties Microstructure and Processing* **2005**, *403*, 182-185.
[38] A. S. Ulihin, A. B. Slobodyuk, N. F. Uvarov, O. A. Kharlamova, V. P. Isupov, V. Y. Kavun, *Solid State Ionics* **2008**, *179*, 1740-1744.
[39] J. T. S. Irvine, D. C. Sinclair, A. R. West, *Adv. Mater.* **1990**, *2*, 132-138.
[40] A. Navrotsky, *J. Mater. Chem.* **2010**, *20*, 10577-10587.
[41] Z. Y. Wen, Z. H. Gu, X. H. Xu, X. J. Zhu, *J. Nuclear Mater.* **2004**, *329*, 1283-1286.

[42] J. Mizusaki, H. Tagawa, K. Saito, K. Uchida, M. Tezuka, *Solid State Ionics* **1992**, *53*, 791-797.
[43] M. Mizuhata, Y. Harada, G. J. Cha, A. B. Beleke, S. Deki, *J. Electrochem. Soc.* **2004**, *151*, E179-E185.
[44] K. Kreuer, *Annual Rev. Mater. Res.* **2003**, *33*, 333-359.
[45] R. Haugsrud, T. Norby, *Nat. Mater.* **2006**, *5*, 193-196.
[46] L. Zhang, R. Lan, A. Kraft, M. T. Wang, S. W. Tao, *Electrochem. Commun.* **2010**, *12*, 1589-1592.
[47] S. W. Tao, J. Canales-Vázquez, J. T. S. Irvine, *Chem. Mater.* **2004**, *16*, 2309-2316.
[48] V. V. Kharton, F. M. B. Marques, A. Atkinson, *Solid State Ionics* **2004**, *174*, 135-149.
[49] S. W. Tao, J. T. S. Irvine, *Adv. Mater.* **2006**, *18*, 1581-1584.
[50] G. Ma, F. Zhang, J. Zhu, G. Y. Meng, *Chem. Mater.* **2006**, *18*, 6006-6011.
[51] L. Zhang, R. Lan, C. T. Petit, S. W. Tao, *Inter. J. Hydrogen Energy* **2010**, *35*, 6934-6940.

Figure captions

Table 1. Lattice parameters of the γ-$LiAlO_2$ and α-$LiFeO_2$ phases in the composite materials derived from the patterns shown in Figure 1.

Figure 1. The XRD pattern of the sample after fired in air at 900 ° (A), after conductivity measurements (B) and after the fuel cell measurements (C).

Figure 2. SEM imagines of the cross-section of the $LiFeO_2$-$LiAlO_2$ composite samples before (A) and after (B) the fuel cell measurements.

Figure 3. The conductivity of stability $LiFeO_2$-$LiAlO_2$ composite at 700 °C in air and dry 5%H_2/Ar (A) and the conductivity at different temperatures (B).

Figure 4. A.c. impedance spectra of the $LiFeO_2$-$LiAlO_2$ composite in air at 700 °C recorded at 0, 60 and 135 minutes respectively (A, B) and the impedance at 700, 610 and 512 °C (C and D).

Figure 5. Thermogravimetric analysis of the nominal '$LiFe_{0.7}Al_{0.3}O_2$' sample in air and 5%H_2/Ar.

Figure 6. A.c. impedance spectra of the $LiFeO_2$-$LiAlO_2$ composite in 5%H_2/Ar at 700 °C recorded at 0, 240 and 480 minutes respectively (A) and the enlarged plot at high frequency (B).

Figure 7. Measured and theoretical voltage of concentration cell O_2 , Ag|$LiFe_{0.7}Al_{0.3}O_2$|Ag, air concentration cell (A), 5%H_2/Ar, Ag |$LiFe_{0.7}Al_{0.3}O_2$|Ag, H_2 (B) and O_2, Ag |$LiFe_{0.7}Al_{0.3}O_2$|Ag, H_2 (C) on heating and cooling.

Figure 8. OCV change against temperature for a H_2/air fuel cell using Ag electrodes.

Figure 9. The H_2/air fuel cell performance at 650 °C at different cycles (A); the fuel cell performance at different temperatures (B).

Figure 10. The a.c. impedance spectra of the H_2/air fuel cell at different temperatures when measured at OCV (A) and the enlarged area at low resistance (B).

Table 1. Lattice parameters of the γ-$LiAlO_2$ and α-$LiFeO_2$ phases in the composite materials derived from the patterns shown in Figure 1.

Samples	γ-$LiAlO_2$ phase			α-$LiFeO_2$ phase	
	a (Å)	*c* (Å)	*V* (Å^3)	*a*(Å)	*V* (Å^3)
$LiFeO_2$-$LiAlO_2$	5.1992(8)	6.2734(18)	169.58(6)	4.1494(2)	71.44(1)
After conductivity measurements	5.1782(3)	6.2734(6)	168.21(2)	4.1555(1)	71.76(1)
After fuel cell measurements	5.1829(4)	6.2810(10)	168.72(3)	4.1536(1)	71.66(1)

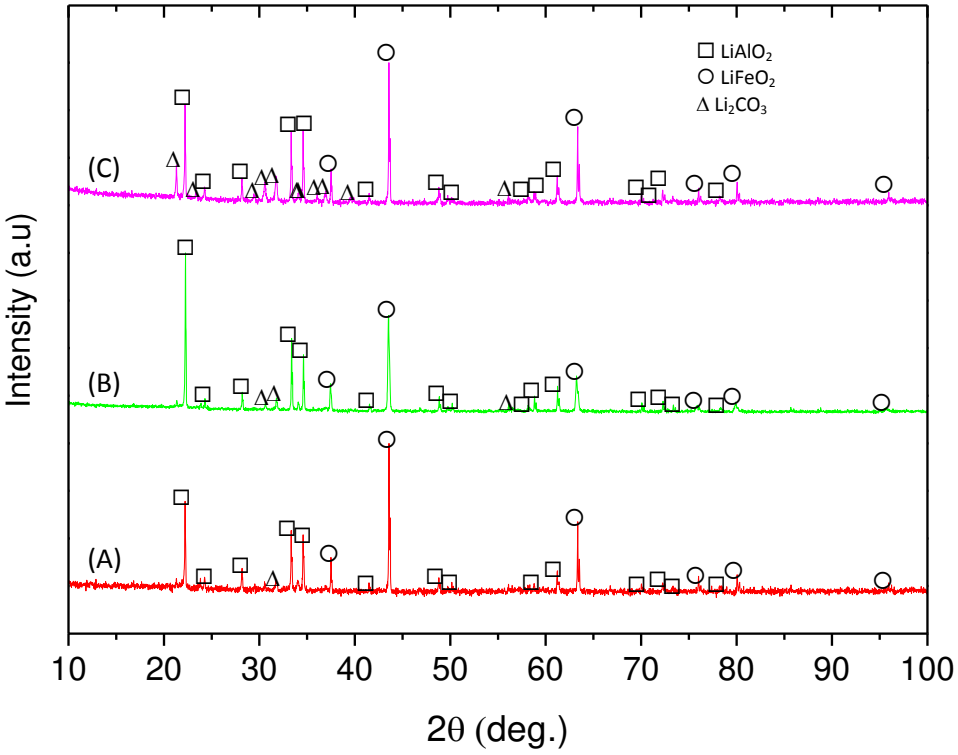

Figure 1. The XRD pattern of the $LiFeO_2$-$LiAlO_2$ composite sample after fired in air at 900 ° (A), after conductivity measurements (B) and after the fuel cell measurements (C).

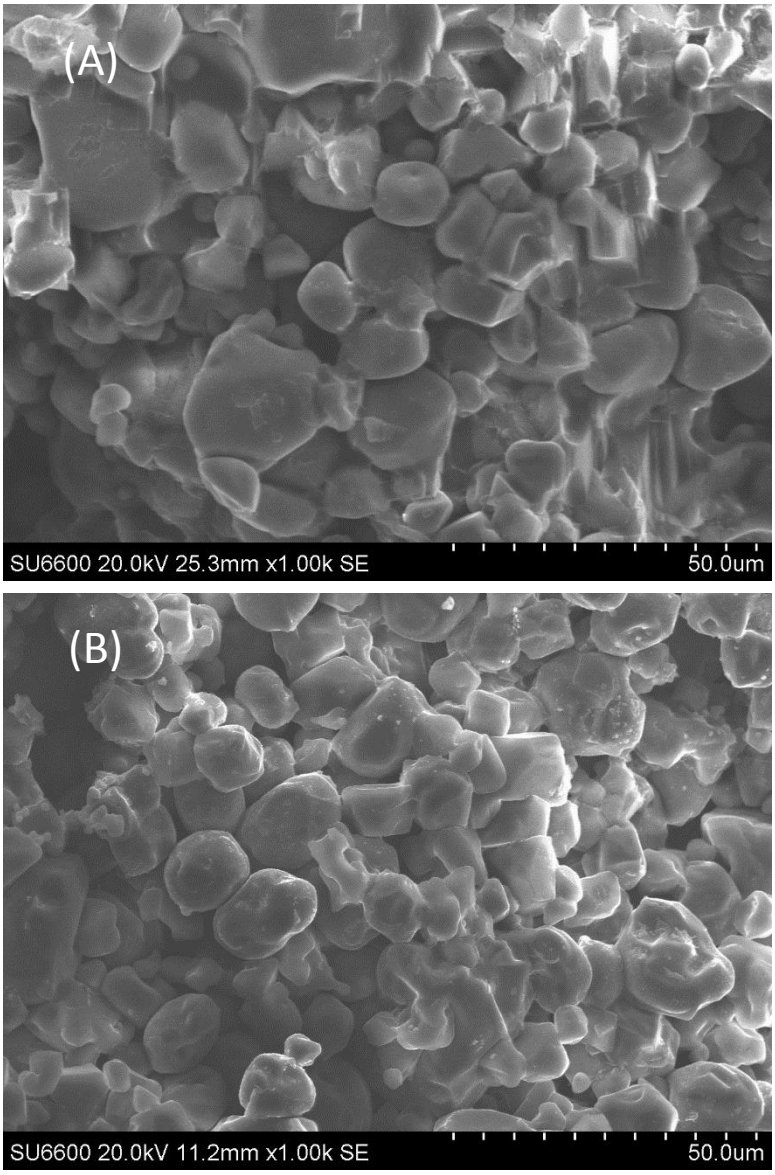

Figure 2. SEM imagines of the cross-section of the $LiFeO_2$-$LiAlO_2$ composite samples before (A) and after (B) the fuel cell measurements.

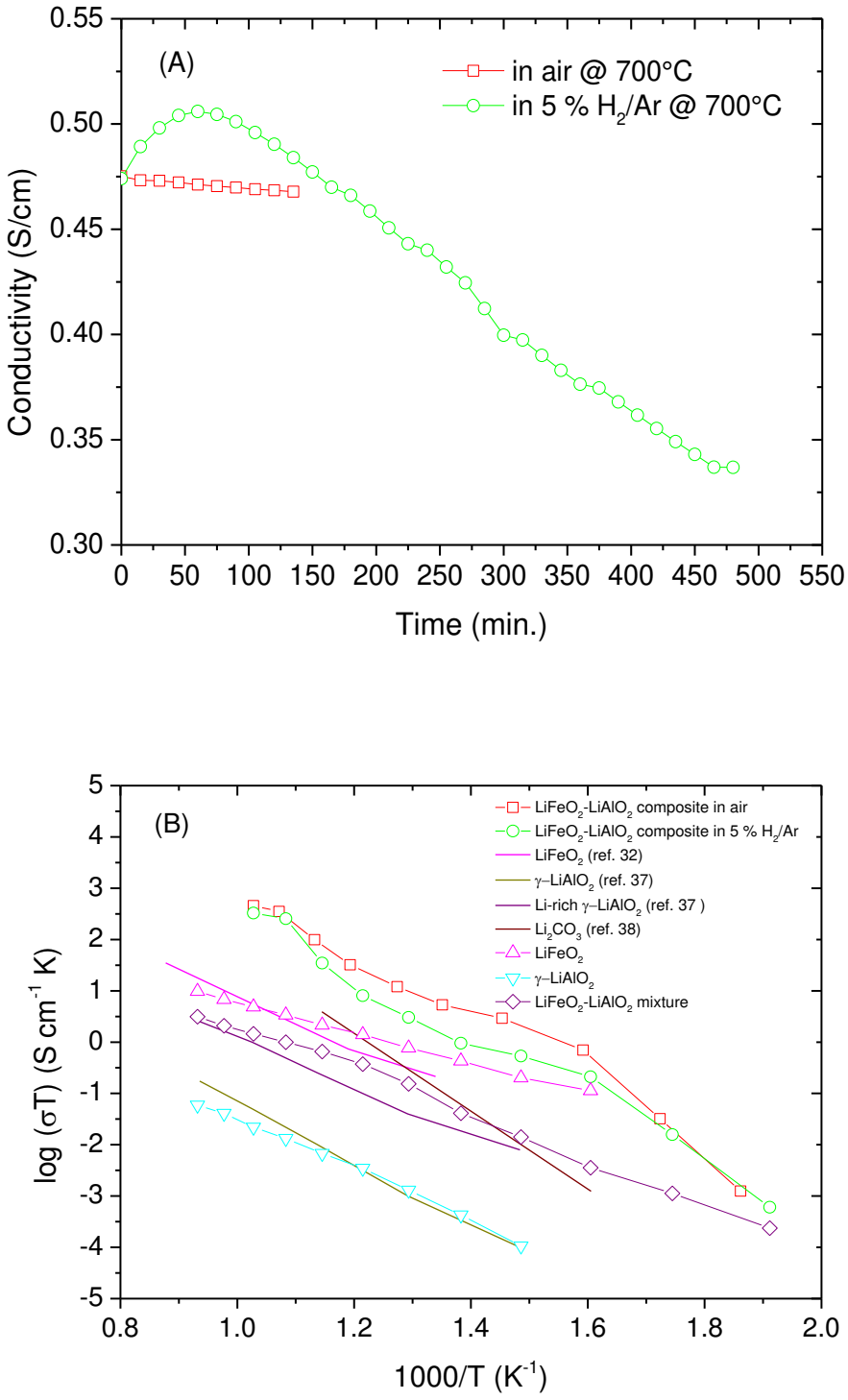

Figure 3. The conductivity of stability $LiFeO_2$-$LiAlO_2$ composite at 700 °C in air and dry 5%H_2/Ar (A) and the conductivity at different temperatures (B).

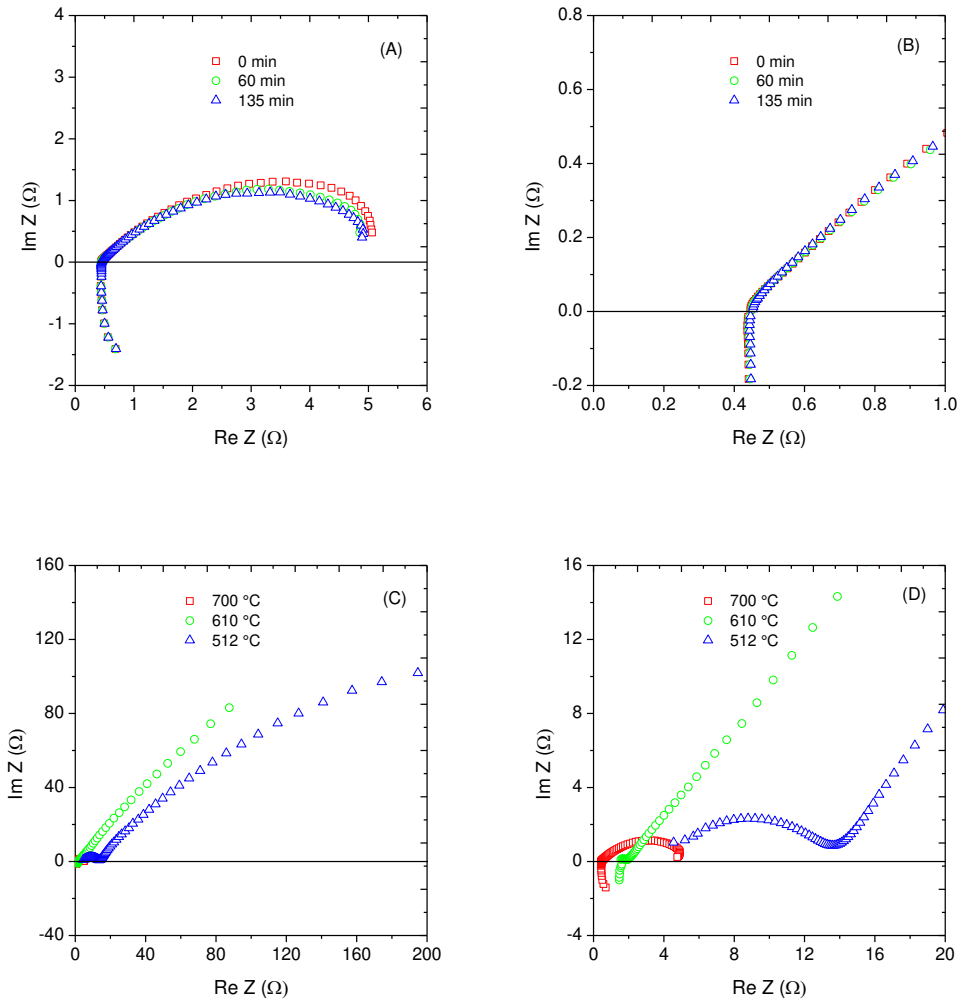

Figure 4. A.c. impedance spectra of the $LiFeO_2$-$LiAlO_2$ composite in air at 700 °C recorded at 0, 60 and 135 minutes respectively (A, B) and the impedance at 700, 610 and 512 °C (C and D).

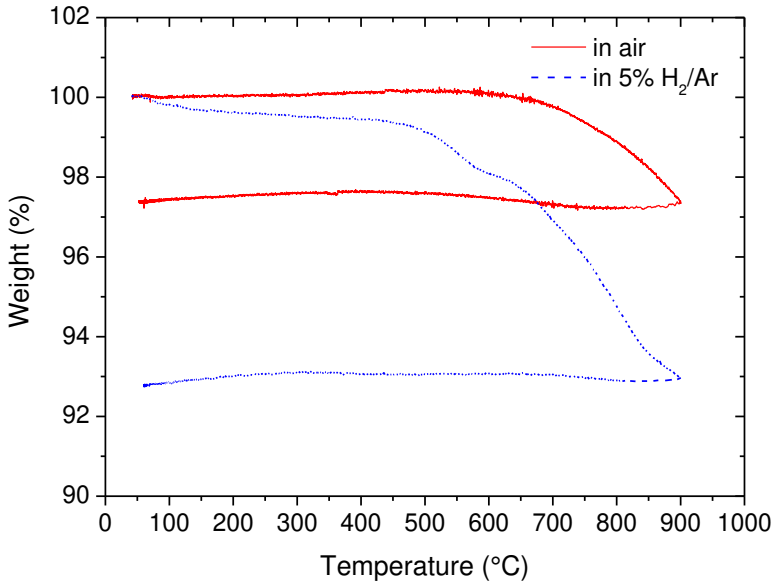

Figure 5. Thermogravimetric analysis of the nominal '$LiFe_{0.7}Al_{0.3}O_2$' sample in air and 5%H_2/Ar.

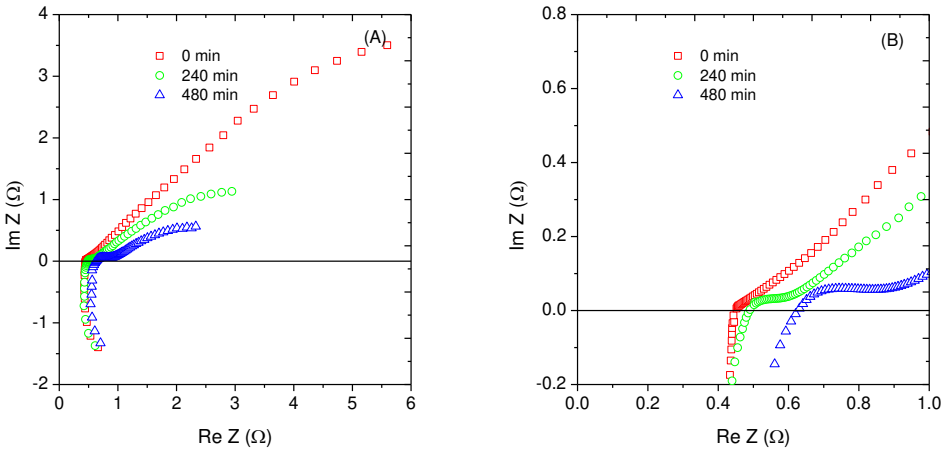

Figure 6. A.c. impedance spectra of the $LiFeO_2$-$LiAlO_2$ composite in 5%H_2/Ar at 700 °C recorded at 0, 240 and 480 minutes respectively (A) and the enlarged plot at high frequency (B).

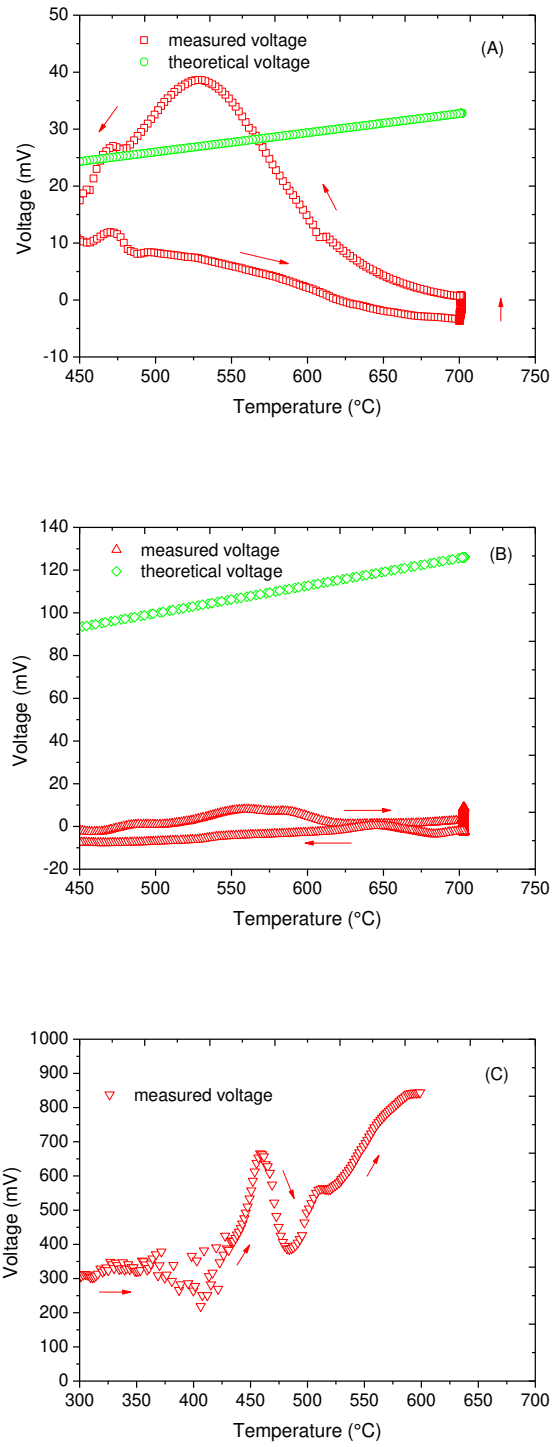

Figure 7. Measured and theoretical voltage of concentration cell O_2 , Ag|$LiFe_{0.7}Al_{0.3}O_2$|Ag, air concentration cell (A), 5%H_2/Ar, Ag |$LiFe_{0.7}Al_{0.3}O_2$|Ag, H_2 (B) and O_2, Ag |$LiFe_{0.7}Al_{0.3}O_2$|Ag, H_2 (C) on heating and cooling.

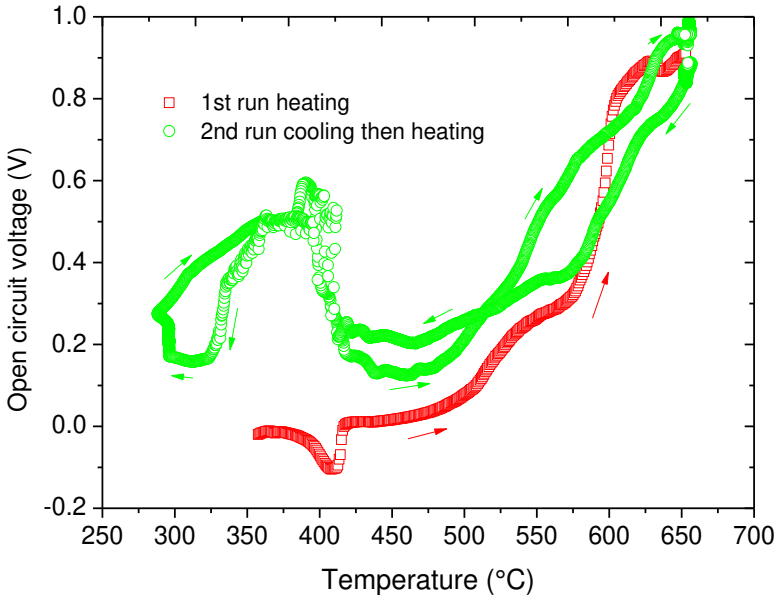

Figure 8. OCV change against temperature for a H_2/air fuel cell using Ag electrodes.

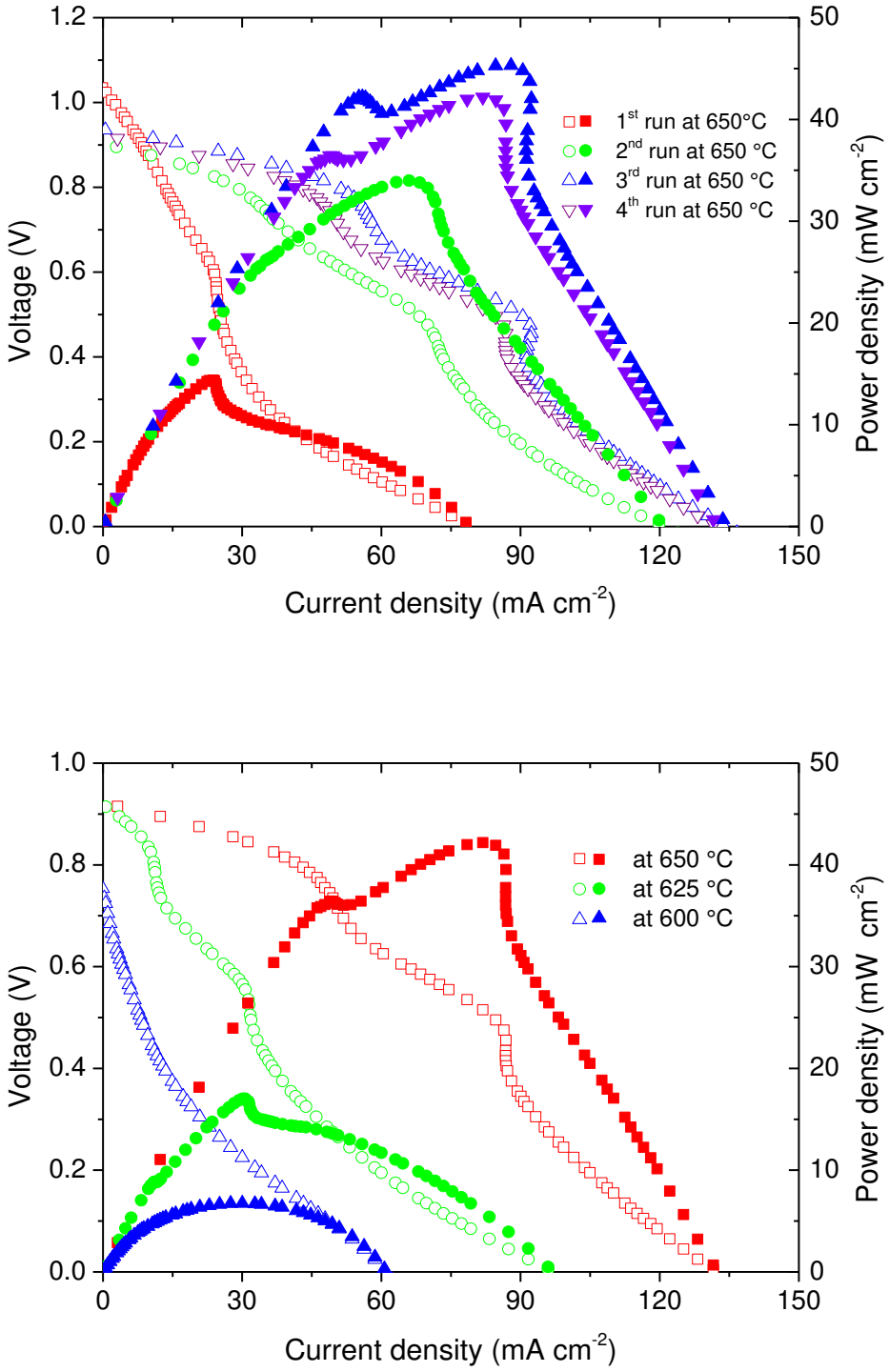

Figure 9. The H_2/air fuel cell performance at 650 °C at different cycles (A); the fuel cell performance at different temperatures (B).

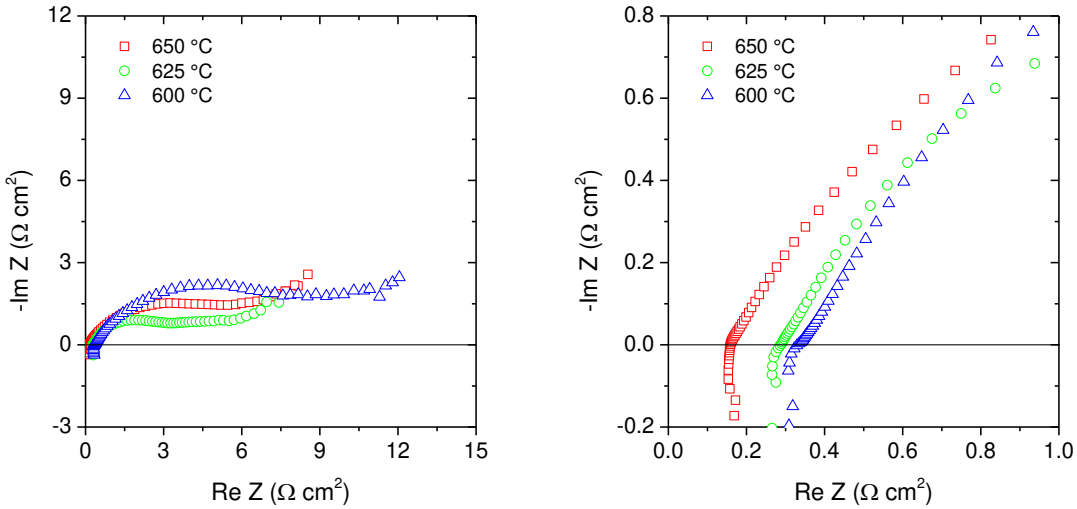

Figure 10. The a.c. impedance spectra of the H_2/air fuel cell at different temperatures when measured at OCV (A) and the enlarged area at low resistance (B).

Supporting Information for:

High ionic conductivity in a $LiFeO_2$-$LiAlO_2$ composite under H_2/air fuel cell condition

Rong Lan and Shanwen Tao*

Department of Chemical & Process Engineering, University of Strathclyde, Glasgow G1 1XJ, UK

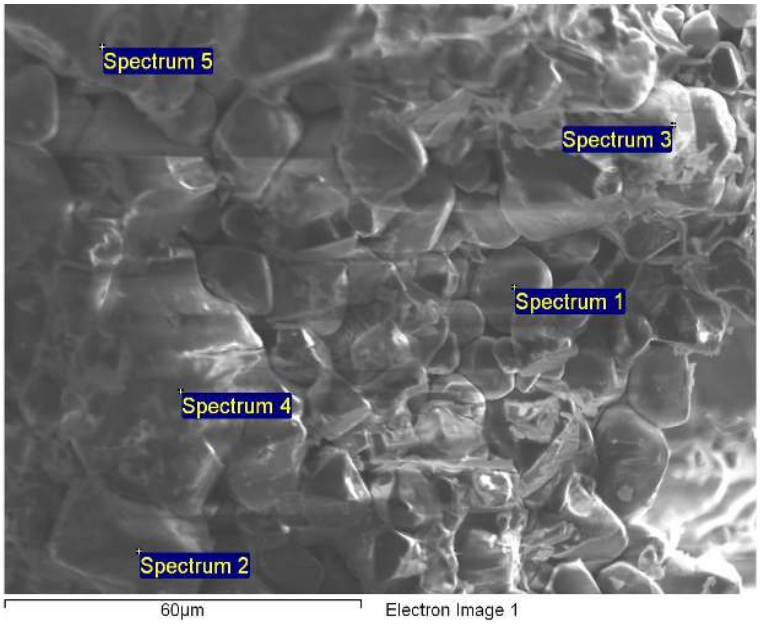

Processing option : All elements analysed (Normalised)

Spectrum	In stats.	O	Al	Fe	Total
Spectrum 1	Yes	1.90	0.49	97.61	100.00
Spectrum 2	Yes	39.66	1.97	58.37	100.00
Spectrum 3	Yes	51.96	2.62	45.42	100.00
Spectrum 4	Yes	56.15	42.00	1.85	100.00
Spectrum 5	Yes	7.41	0.35	92.24	100.00
Mean		31.42	9.49	59.10	100.00
Std. deviation		25.24	18.20	38.88	
Max.		56.15	42.00	97.61	
Min.		1.90	0.35	1.85	

All results in weight%

Figure S1 The EDS analysis of the $LiFeO_2$-$LiAlO_2$ composite.